An Approach to Increasing Yields of a Sunscreen Compound in Recombinant Yeast

by
Van Anh Vu

A THESIS

submitted to

Oregon State University

University Honors College

in partial fulfillment of
the requirements for the
degree of

Honors Baccalaureate of Science in BioHealth Sciences
(Honors Scholar)

Honors Baccalaureate of Arts in International Studies
(Honors Scholar)

Presented May 20, 2016
Commencement June 2016

AN ABSTRACT OF THE THESIS OF

Van Anh Vu for the degree of Honors Baccalaureate of Science in BioHealth Sciences and Honors Baccalaureate of Arts in International Studies presented on May 20, 2016. Title: An Approach to Increasing Yields of a Sunscreen Compound in Recombinant Yeast.

Abstract approved: _____

Alan Bakalinsky

The yeast *Saccharomyces cerevisiae*, commonly used in winemaking, baking, and brewing, also serves as a host for the production of therapeutically valuable pharmaceuticals. Recently, the Bakalinsky laboratory constructed a recombinant yeast strain expressing two zebrafish (*Danio rerio*) genes in order to produce a UV-protective "sunscreen" compound called gadusol. An antioxidant with sunscreen activity and commercial potential, gadusol is derived from the pentose phosphate pathway (PPP) intermediate sedoheptulose 7-phosphate (S7P) that occurs naturally in yeast. Because it is likely that increased S7P levels can increase gadusol yields in yeast, a method was sought to quantify glucose flux through the PPP relative to flux through glycolysis, the main glucose-consuming pathway in this organism. This thesis project developed such a method and used it to compare glucose flux in the gadusol-producing yeast relative to an isogenic, non-gadusol-producing control strain. By feeding cells labeled $^{13}C_1$-glucose and measuring $\delta^{13}C$ of CO_2 produced by yeast, using isotope ratio mass spectrometry (IRMS), glucose flux through the PPP was found to be 2.5% higher in the gadusol-producing yeast than in the control strain. This method will provide a simple means of monitoring the effectiveness of cultural and genetic interventions to increase glucose flux through the PPP.

Key Words: Yeast, pentose phosphate pathway (PPP), glucose flux, gadusol, sunscreen

Corresponding e-mail address: vananh94@gmail.com

An Approach to Increasing Yields of a Sunscreen Compound in Recombinant Yeast

by
Van Anh Vu

A THESIS

submitted to

Oregon State University

University Honors College

in partial fulfillment of
the requirements for the
degree of

Honors Baccalaureate of Science in BioHealth Sciences
(Honors Scholar)

Honors Baccalaureate of Arts in International Studies
(Honors Scholar)

Presented May 20, 2016
Commencement June 2016

Honors Baccalaureate of Science in BioHealth Sciences and Honors Baccalaureate of Arts in International Studies project of Van Anh Vu presented on May 20, 2016.

APPROVED:

Alan Bakalinsky, Mentor, representing Food & Science Technology

Jennifer McKay, Committee Member, representing College of Earth, Ocean, and Atmospheric Sciences

Kerry Thomas, Committee Member, representing International Degree Program

Toni Doolen, Dean, University Honors College

I understand that my project will become part of the permanent collection of Oregon State University, University Honors College. My signature below authorizes release of my project to any reader upon request.

Van Anh Vu, Author

Acknowledgements

I would like to thank Alan Bakalinsky for serving as my mentor and guiding me throughout this entire thesis project. Thank you for your patience, dedication, and endless support. I couldn't have done it without you!

I would also like to thank Jennifer McKay for allowing me to use her IRMS instruments for my data collection (during the weekends), and for serving as my thesis committee member.

Thank you to Kerry Thomas, advisor of the International Degree Program, for serving as the third thesis committee member.

I want to thank Astrid Stuckelberger from Switzerland, author of *Anti-Ageing Medicine: Myths and Chances*, for providing me with the background knowledge for the international component of my thesis project.

My lovely lab colleagues, Garrett Holzwarth, Allen Yoshinaga, and Elizabeth Kim, I couldn't have made it without your sense of humor. Garrett and Allen, thank you for being so patient in teaching me the necessary lab skills, and being beyond helpful during the difficult times of research. Elizabeth, I'm so glad there's another woman in the lab.

Sist men ikke minst, tusen takk til dere Pappa og Mamma for alt dere har gjort for meg. Kjempe glad i dere, og vises snart!

TABLE OF CONTENTS

1. Literature Review

1.1. The Yeast *Saccharomyces cerevisiae*

The yeast *S. cerevisiae* is a single-celled fungus, domesticated unknowingly by humans thousands of years ago because of the essential role it plays in the production of bread, wine, beer and other fermented foods. This organism is also widely used to produce beverage and fuel ethanol, and serves as a host for the production of recombinant proteins used in the food industry and in healthcare. As an experimentally tractable eukaryotic organism, *S. cerevisiae* continues to serve as a powerful experimental model for the study of a wide variety of biological processes as it shares many of the functions essential for life in higher organisms (e.g., humans), while offering practical advantages for laboratory studies.

This species is a vigorous fermenter of sugar, reproduces by multilateral budding, and consists of 3 cells types: **a** and α haploids, and an **a**/α diploid. As an *Ascomycete*, it forms gametes or ascospores at the end of meiosis in a structure called an ascus. Unlike the gametes of plants and animals, the germinated haploid spores of *S. cerevisiae* are able to grow vegetatively (mitotically). The diploid stage is restored when haploids of the opposite mating type are mixed, resulting in mating (**Figure 1**).

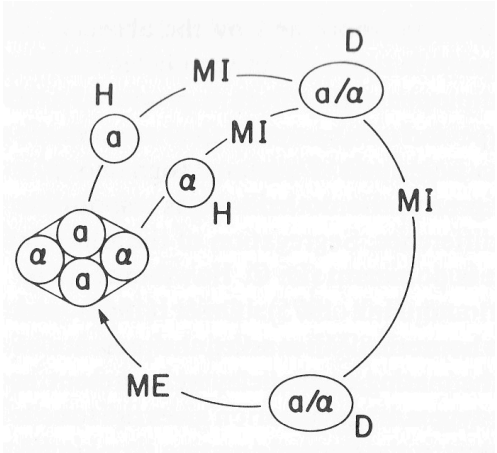

Figure 1. Life cycle of *S. cerevisiae* involves an alternation of haploid and diploid cell types.
D = diploid; H = haploid, ME = meiosis; and MI = mitosis. Three cell types: a, alpha, and a/alpha.

1.2. Central Carbon Metabolism in Yeast

Although *S. cerevisiae* is capable of aerobic respiration, it prefers to metabolize glucose via alcoholic fermentation, in spite of lower energy and biomass yields per unit mass of glucose than during aerobic respiration (**Figure 2**). During fermentation, glucose is converted to carbon dioxide and ethanol in the absence of external electron acceptors (e.g., oxygen). Even though the net oxidation state of the substrate glucose is the same as that of the sum of the products (ethanol and carbon dioxide), the internal rearrangements result in oxidation of some of the carbons and reduction of others. A small amount of the energy generated in the rearrangements is captured via substrate-level phosphorylation – formation of high-energy intermediates – that ultimately results in the generation of two molecules of ATPs per molecule of glucose fermented (Berg *et al.,* 2012). Aerobic respiration, on the other hand, involves the complete oxidation of glucose to carbon dioxide and water with oxygen serving as the electron acceptor. Although the theoretical ATP yield from respiration is about 15 times greater than fermentation, *S. cerevisiae* preferentially ferments glucose. A number of possibilities could explain this preference.

In its native, sugar-rich environment (e.g., rotting fruit), the organism has no need to conserve carbon or to use it efficiently as other nutrients are typically limiting (e.g., nitrogen or phosphorus). Yeast grows more rapidly when it ferments than when it respires glucose, which could provide an advantage over other microbes in the same ecological niche. Yeast also has a much higher tolerance for ethanol than its microbial competitors, and therefore, production of alcohol by fermentation may be a way of inhibiting their growth. Fermentative metabolism generates less oxidative stress than aerobic respiration, and hence less energy and resources need to be devoted to coping mechanisms. Finally, the actual energy yield from the respiration of glucose may be overstated due to the need to maintain a functional mitochondria, an electron transport chain, and other respiration-specific activities not required during fermentative growth.

In addition to providing energy, fermentation also produces the biochemical building blocks for the synthesis of new cells (e.g., pyruvate, phosphoenolpyruvate). During both fermentation and respiration, some glucose is always metabolized via the pentose phosphate pathway (PPP), which provides reducing power in the form of NADPH needed for biosynthetic reactions, and intermediates (e.g., ribose 5-phosphate, erythrose 4-phosphate) needed to make nucleotides, histidine, and aromatic amino acids (Fraenkel *et al.,* 1982). The end products of the PPP (fructose 6-phosphate and glyceraldehyde 3-phosphate) re-enter glycolysis for further catabolism (**Figure 3**).

When yeast respires glucose, the pyruvate generated during glycolysis is converted to acetyl-CoA instead of ethanol (**Figure 2**). The acetyl-CoA enters the citric acid cycle (CAC) and is completely oxidized to carbon dioxide and water leading to a theoretical yield of about 30 ATPs per glucose (Berg *et al.,* 2012). During respiratory growth, some intermediates made in the CAC are also used to synthesize compounds needed to make new cells (e.g., fatty acids, amino acids, sterols). During fermentative growth, the CAC operates as a partial cycle, supplying the same essential intermediates but without the accompanying high-energy output (Berg *et al.,* 2012).

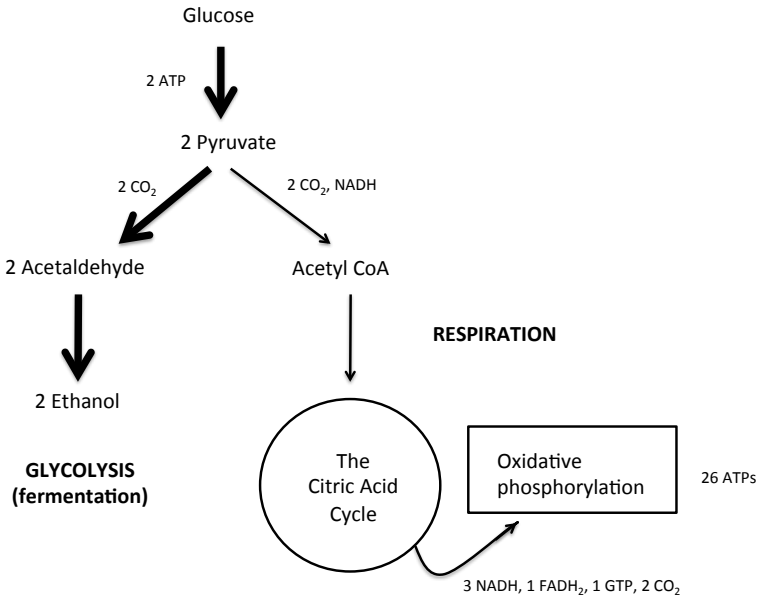

Figure 2. Alcoholic fermentation and aerobic respiration in yeast. Although yeast obtains approximately 15 times more energy through respiration than fermentation, it still prefers to ferment glucose. The extent of carbon flow is represented by the size of the arrows.

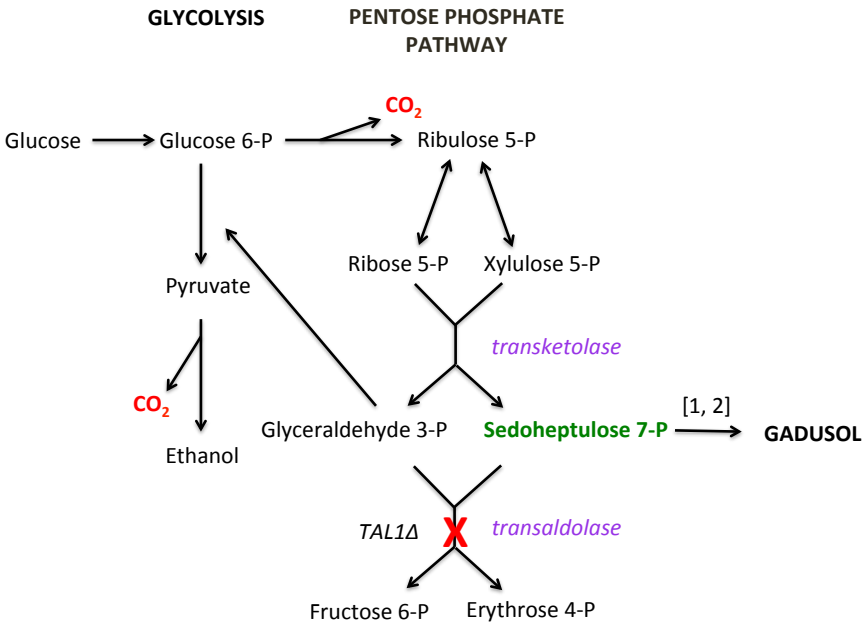

Figure 3. Abbreviated glycolytic and the pentose phosphate pathway (PPP) in *S. cerevisiae*. Glyceraldehyde 3-phosphate generated from ribose 5-phosphate via the PPP can re-enter glycolysis. Gadusol is derived from the PPP intermediate sedoheptulose 7-phosphate in two steps catalyzed by zebrafish 2-epi-5-epi valiolone synthase (EEVS) and methyl transferase oxidoreductase (MT-Ox), referred to as [1,2] in the figure.

1.3. Experimental Problem

The Bakalinsky laboratory recently constructed a recombinant strain of the yeast *S. cerevisiae* that expresses two zebrafish genes (EEVS and MT-Ox) and produces about 20 mg/liter of a naturally-occurring ultraviolet light (UV)-absorbing compound known as gadusol (Osborn *et al.,* 2015). This "sunscreen" compound is believed to play an important role in protecting the organisms in which it occurs naturally from the damaging effects of UV irradiation. Because none of the natural sources of this compound – fish, amphibians, reptiles, and birds – can provide sufficient quantities for potential therapeutic use, the widely used industrial microorganism *S. cerevisiae* was chosen to produce the compound. The constructed yeast strain was chosen for demonstration purposes – not optimal genetic background (genotype) – and therefore it is likely that levels can be greatly increased by undertaking a systematic effort to optimize genotype and growth conditions for gadusol overproduction. A review of the literature on the factors that control production of the naturally occurring gadusol precursor in yeast, sedoheptulose 7-phosphate – an intermediate formed in the PPP, suggests that straight forward interventions may greatly enhance yields.

The specific goal of this thesis project was to develop a simple method to determine glucose flux through the pentose phosphate pathway in order to assess the effect of genetic or cultural interventions on gadusol yields in glucose-grown yeast cultures.

Metabolic Flux Analysis

Metabolic flux analysis (MFA) is a standard method to quantify central carbon metabolism as carbon flow or flux during cell growth. The requirements of the method include 1) a stoichiometric model that accounts for all the major intracellular reactions in the organism of interest, 2) growing cells at steady-state, 3) measurements of carbon inputs (e.g., glucose) and outputs (e.g., ethanol, cell mass) during steady-state growth; and 4) measurements of the

concentration of selected metabolic intermediates (Toya *et al*., 2011; Nissen *et al*., 1997). The stoichiometric model is used to develop a matrix to account for carbon flow. Fluxes are determined from mass balancing around the intracellular metabolites based on the measured inputs, outputs, and concentrations of metabolic intermediates. The approach is powerful but requires significant effort in two areas. First, experimental effort is needed to grow microbial cultures and to quantify a number of metabolites, and second, mathematical expertise is needed to model the data in order to generate accurate intracellular carbon fluxes.

Because such an effort was beyond the scope of an Honors Thesis project, a simpler alternative was developed. The alternative exploited the fact that the CO_2 produced in the PPP is derived exclusively from the C_1 carbon of glucose (Katz *et al.,* 1955), whereas the CO_2 produced in glycolysis is generated from the C_3 and C_4 carbons (**Figure 4**). Thus, by measuring $^{13}CO_2/^{12}CO_2$ ratios in the headspace above yeast cultures fed $^{13}C_1$-glucose, we reasoned that it would be possible to determine flux in a control strain and in any strain subjected to an experimental intervention. As a first estimate, the intervention would be considered helpful if the $^{13}CO_2/^{12}CO_2$ ratio was found to increase in the experimental culture relative to the control. A sensitive analytical technique – isotope-ratio mass spectrometry (IRMS) – was chosen to measure $^{13}CO_2/^{12}CO_2$ ratios.

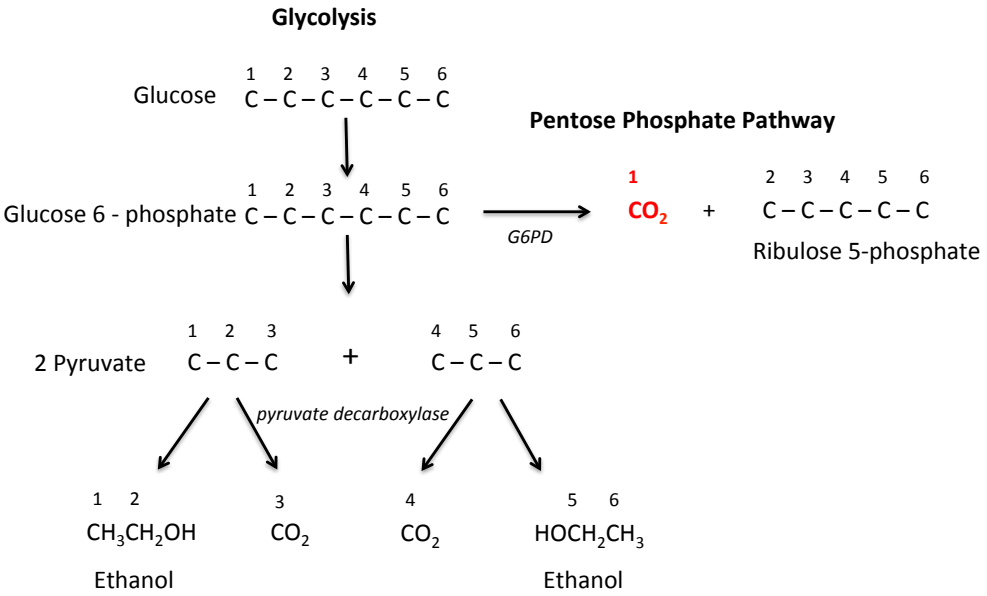

Figure 4. Carbon tracing of glucose metabolized in yeast via glycolysis and the PPP. The numbering indicates the carbon atoms in glucose.

Measuring Glucose Flux

Several procedures, including different types of nuclear magnetic resonance (NMR)- and mass spectrometry (MS)-based techniques, can detect the differences of isotopomers (e.g., isotopic isomers $^{13}C_1$-glucose versus $^{13}C_2$-glucose) to gain information about the intracellular labeling state of the system. For MFA, liquid-chromatography mass spectrometry (LC-MS) is typically used to separate and quantify metabolic intermediates. In contrast, gas-chromatography mass spectrometry (GC-MS) is commonly used for volatile metabolites. In one study, GC-MS was used to determine $^{13}CO_2/^{12}CO_2$ ratios in ^{13}C-urea breath test samples for the diagnosis of *Helicobacter pylori* infection (Jordaan *et al*., 2008). Presumptive ulcer patients were given ^{13}C-urea tablets before breath sample collection because humans lack a unique urease enzyme found in *H. pylori*. Only patients (ulcer-associated) with *H. pylori* infection were expected to generate $^{13}CO_2$. Unfortunately, the amount of $^{13}CO_2$ we expect to generate cannot be separated from $^{12}CO_2$ and

quantified by standard GC-MS instrumentation. To overcome this problem, isotope ratio mass-spectrometry (IRMS) was chosen to quantify $^{13}CO_2/^{12}CO_2$ levels produced by yeast.

In order to recognize why GC-MS is less sensitive than IRMS, we must understand the fundamental functions of each detector. GC-MS is an analytical method that combines gas chromatography and mass spectrometry. Gas chromatography is a technique that incorporates a capillary column consisting of a stationary liquid phase and mobile gas phase that separates volatile components in a mixture based on differential affinity for the stationary phase. A beam of electrons ionizes the separated gas-phase solutes before they enter the mass spectrometer. Mass spectrometry in GC-MS uses a quadrupole mass analyzer, which consists of four adjustable, cylindrical metal rods set parallel to one another (**Figure 5**). The quadrupole mass analyzer acts as a "mass filter," set to pass ions having a selected mass-to-charge ratio (m/z). The ions are separated based on the stability of their trajectories in the oscillating electrical field applied to the rods (Zabielski *et al*., 2013). Ions that do not have a straight trajectory will collide with the rods, and never reach the detector. GC-MS only detects one isotope at a time. The standard columns used in GC analysis cannot separate $^{13}CO_2$ from $^{12}CO_2$, and without this separation, detection is problematic.

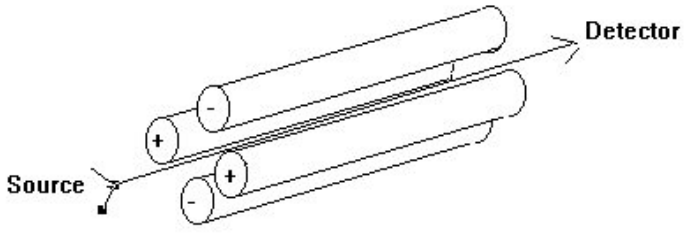

Figure 5. Schematic of a quadrupole mass analyzer.

The method chosen for the present study, IRMS, on the other hand, is a specialized technique of mass spectrometry that can measure the relative isotopic abundance of CO_2 in a mixture using a magnetic analyzer. As in GC-MS, a gas sample is first fed into an ionization chamber to become ionized by a beam of electrons. The resulting ionized gas is accelerated and focused as a beam through the magnetic analyzer where a magnetic field is applied in a direction perpendicular to the direction of the ions. This separates the ions based on mass-to-charge ratio (m/z). After passing through the electromagnet, the trajectory of the ions with a lighter m/z bends at a smaller angle. Faraday detectors, which generate electrical signals that are proportional to the number of ions detected, collect the separated ions, allowing for the quantification of isotopic ratios (Muccio *et al*., 2008) (**Figure 6**). This type of analyzer is superior to the quadrupole type for three reasons: 1) no prior isotope separation is needed, 2) the instrument can be set up to collect isotopomers of the same atom, and 3) the magnetic analyzer gives high-quality peak shapes with higher resolution and higher sensitivity than the quadrupole mass analyzer.

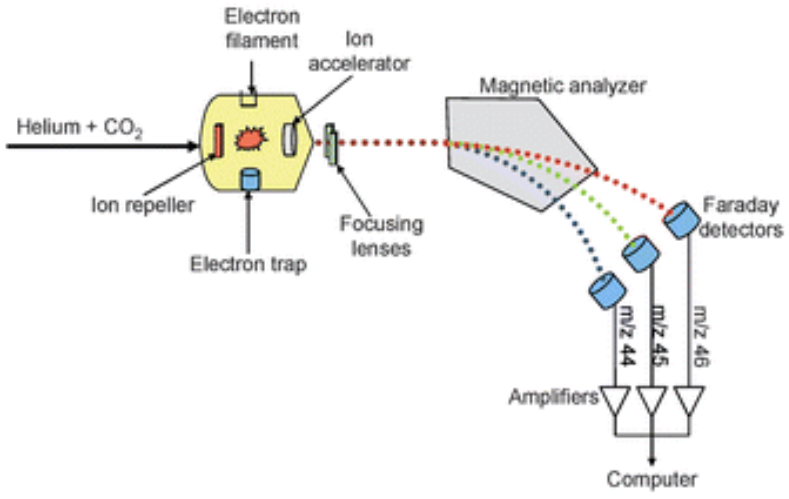

Figure 6. The internal layout of the IRMS (Muccio *et al*., 2008).

2. Materials and Methods

2.1. Yeast Strains

Yeast strains and genotypes are listed in Table 1. Both strains contained a knockout allele of *TAL1* gene at the step in the pentose phosphate pathway that catalyzes the formation of fructose 6-phosphate and erythrose 4-phosphate from glyceraldehyde 3-phosphate and sedoheptulose 7-phosphate (**Figure 3**). The gadusol-producing strain (Gad+) harbors two yeast expression vectors, pXP416 and pxP420 carrying zebra fish MT-Ox and EEVS genes (cDNAs), respectively, needed to make gadusol from sedoheptulose 7-phosphate. The control strain, in contrast, carries only the empty expression vectors.

Table 1. Yeast strains and their genotypes

Yeast Strains	Genotype
Gad+	BY4742 *MATα tal1Δ::KanMX4 his3Δ1 leu2Δ0 lys2Δ0 trp1Δ::URA3*/ pXP416-MT-Ox *HIS3*, pXP420-EEVS *TRP1*
Control	BY4742 *MATα tal1Δ::KanMX4 his3Δ1 leu2Δ0 lys2Δ0 trp1Δ::URA3*/ pXP416, pXP420

2.2. Yeast Media and Growth Conditions

Liquid cultures of the Gad+ and control strains were begun by inoculating a standard synthetic yeast medium, yeast nitrogen base (YNB) + 2% glucose + 60 mg/l leucine + 60 mg/l lysine, with cells taken from the same agar-based medium stored at 4°C for no more than 2 weeks. The cultures were grown aerobically in 15-ml test tubes at 30°C and 200 rpm for 24 hours. Growth of the experimental cultures was then initiated by diluting these 24-hour cultures to 10^6 cells/ml into 19 ml of the same medium in triplicate ~23-ml screw-capped vials with rubber septa closures (VWR catalog no. IRS126-0020) containing 2% total glucose of which 2% was $^{13}C_1$-glucose. That is,

every 100 ml of culture contained 1.96 g of unlabeled ^{12}C-glucose and 0.04 g of $^{13}C_1$-glucose. (The empty vials and closures were surface sterilized with 70% ethanol and dried in a sterile laminar flow hood prior to use.) The filled vials contained ~4 ml of headspace. A sterile hypodermic needle (25 gauge) loosely covered with aluminum foil to maintain internal sterility was then inserted into the septa to allow both venting and collection of fermentation volatiles (mostly CO_2, some ethanol and other minor constituents). After approximately 4 to 5 headspace volumes of gas had been vented and cells had begun exponential growth (~22 hours post-inoculation), a 12 ml plastic syringe barrel and plunger were attached to the needle aseptically to allow collection of ~6 ml of fermentation gas (**Figure 7**). The syringes (including needle and plunger) were then removed from the glass vials, and the headspace samples were injected into another set of vials that had been pre-flushed with helium for IRMS analysis. Two 3-ml aliquots from each experimental gas sample were injected into the IRMS to quantify ^{13}C and ^{12}C ratios.

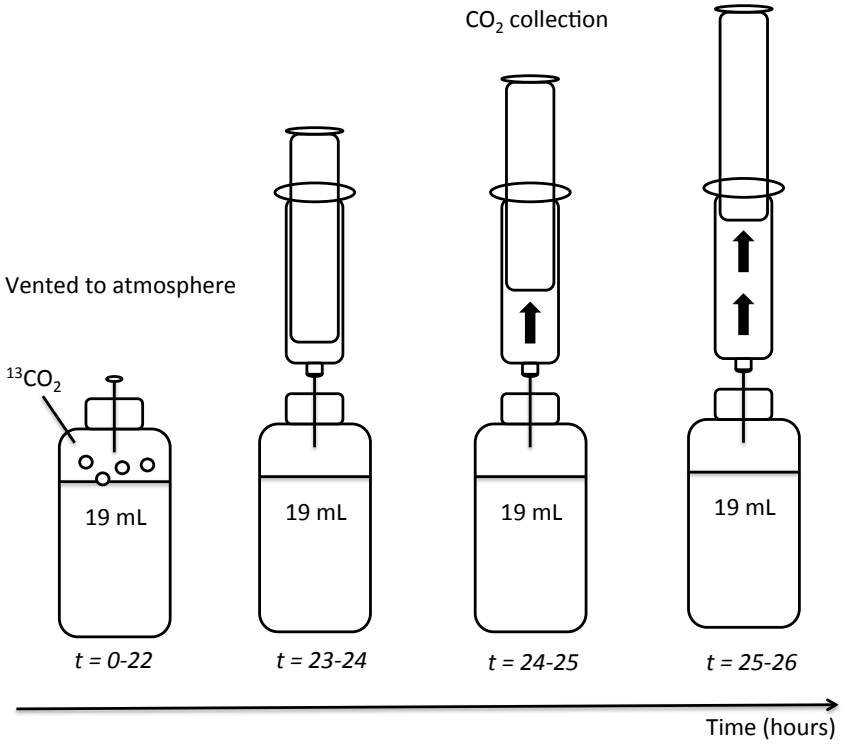

Figure 7. Vessels from which CO_2 was collected during exponential growth of the yeast cultures.

2.3. IRMS Analysis

$^{13}CO_2$ and $^{12}CO_2$ ratios were quantified using a continuous-flow isotope ratio mass spectrometer (IRMS). Samples pre-chilled to 5°C were introduced into a Thermo DeltaV IRMS using a GasBench inlet system. The pre-chilling reduced the volatility of any ethanol present in the headspace, which would otherwise have contributed carbon to the analysis. The mass spectrometer was calibrated against a reference CO_2 gas containing 1.95 parts per thousand $^{13}CO_2$ relative to VPDB, using a defined standard (below). Because all organic matter contains trace amounts of ^{13}C, even the unlabeled ^{12}C-glucose, a standard is needed to quantify the actual amount of ^{13}C. The defined carbon isotope standard is derived from the carbonate shell ($CaCO_3$) – an extinct belemnite (cephalopod) – that contained an actual $^{13}C/^{12}C$ ratio of 0.0112372, historically set to zero. The standard is expressed in delta notation ($\delta^{13}C$), which refers to parts ^{13}C per thousand parts ^{12}C. Because the original standard is no longer available, it has been replaced with another called “Vienna Pee Dee Belemnite (VPDB)” calibrated to the same original ratio. Thus, for example, the reference CO_2 gas used in this experiment is derived from NBS19 calcium carbonate powder via acidification and has a $\delta^{13}C$ of +1.95 per mil VPDB. Thus, this CO_2 standard has a slightly higher natural proportion of $^{13}CO_2$ than the VPDB standard. Substances with a lower $^{13}C/^{12}C$ ratio than the standard are assigned negative $\delta^{13}C$ values.

3. Results and Discussion

3.1. Preliminary Experiments

Preliminary experiments were performed to determine 1) yeast growth rate, 2) appropriate choice of growth vessel, and 3) the amount of $^{13}C_1$-glucose to add to the growth medium.

Yeast growth rate: Determining yeast growth rate was essential as CO_2 samples had to be collected during log phase when cells were growing at steady state, and it was not possible to predict accurately when that period would begin. Growth rate was measured by weighing the growth vessel over a time course as the weight loss corresponded to evolved CO_2, which was vented and proportional to growth. As noted earlier, when yeast ferments, it produces 2 moles of ethanol and 2 moles of CO_2 for every mole of glucose consumed. One practical question that had to be answered was whether the amount of weight that was expected to be lost as evolved CO_2 could be measured accurately using the balance in the laboratory for which 10 mg was the accepted minimum. The calculations in Appendix A show the expected amount of weight loss as a function of glucose consumed was well over this amount. Initially, weights were taken hourly post-inoculation and were plotted on a semi-log scale versus time to determine when log phase growth began. Log phase growth corresponds to maximal growth rate. The control and Gad+ strains were found to have entered log phase at ~20 and ~22 hours post-inoculation, respectively (**Figure 8**).

Choice of growth vessel: An appropriate growth vessel had to be chosen that satisfied the following requirements. Growth vessels had to allow for sampling of the headspace above the yeast culture without altering the gas composition. They also had to be small enough to be held in a small 30°C incubator and portable enough to be moved back and forth to the nearby analytical balance for periodic weighing. Initially, ~25 ml glass vials with crimpable, rubber septa closures were chosen and were surface sterilized with 70% ethanol prior to use. Gas samples collected as described above and analyzed by the IRMS indicated unacceptable leakage of atmospheric N_2 gas. The leakage appeared to be due to the combination of hand crimping of the rubber septa closures and the ability of the ethanol to cause slippage between the septa and outer metal housing. Once screw-capped vials containing rubber septa within the caps themselves were chosen, no further leakage was detected.

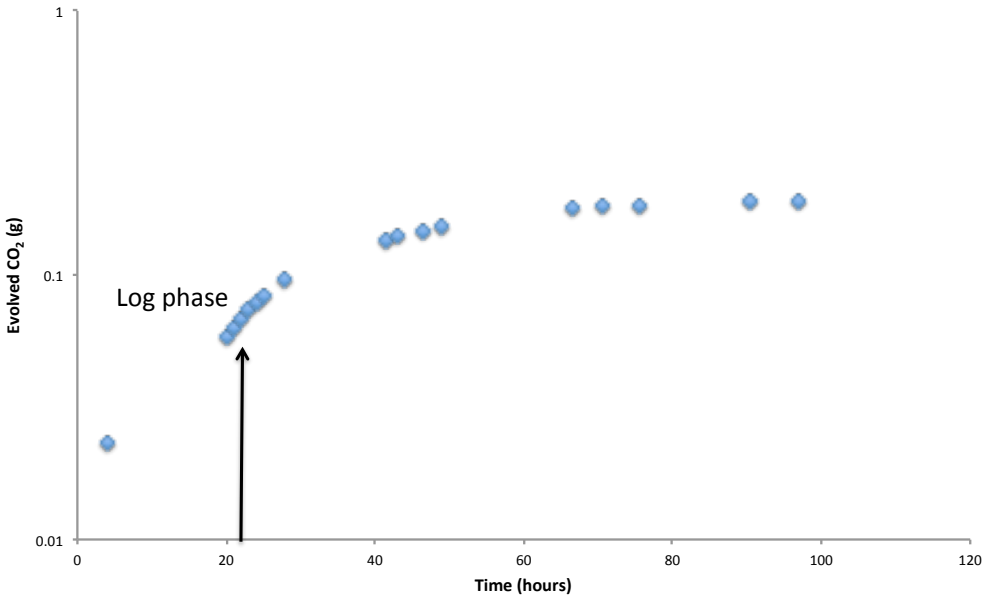

Figure 8a. Yeast growth measured as evolved CO_2 – weight loss – over a time course in the control strain.

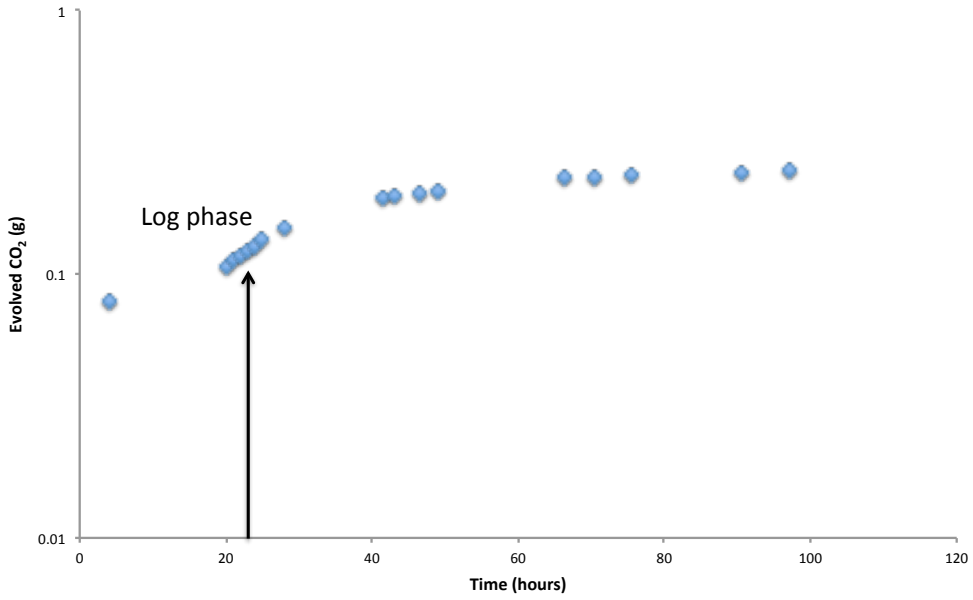

Figure 8b. Yeast growth measured as evolved CO_2 – weight loss – over a time course in the Gad+ strain.

Amount of $^{13}C_1$-glucose to add to the growth medium: Two considerations had to be weighed with respect to how much $^{13}C_1$-glucose to add to the yeast growth medium. Because the isotope ratio mass spectrometer (IRMS) was extremely sensitive, too much label was likely to contaminate the instrument. Further, because $^{13}C_1$-glucose is much more expensive than unlabeled ^{12}C-glucose, the minimum label needed would be optimal. An initial addition of 0.25% $^{13}C_1$-glucose in the total 2% glucose was tested but was found to be too little to distinguish $^{13}CO_2/^{12}CO_2$ ratios between the control and Gad+ strains, -10.54 per mil VPDB and -10.58 per mil VPDB, respectively. Fortuitously, the next addition tested – a 2% $^{13}C_1$-glucose spike – was found to be sufficient.

3.2. $^{13}CO_2/^{12}CO_2$ Determination

Both the control and Gad+ yeast strains were blocked in the pentose phosphate pathway at the transaldolase step (*tal1*Δ) that was expected to lead to an accumulation of S7P and to slow glucose flux (**Figure 3**). Because only the Gad+ strain had a shunt pathway that allowed metabolism of the accumulated S7P to gadusol, we expected that glucose flux through the PPP would be higher in the Gad+ strain than in the control. Based on a theoretical calculation of the expected $^{13}CO_2/^{12}CO_2$ ratio in cells fed $^{13}CO_2$ (Appendix B), we anticipated that the difference in flux between the two strains would be measurable, but could not provide an exact estimate, in part, because of the unknown amount of glucose that would be assimilated into new cell mass versus oxidation to CO_2, and in part, because of the unknown effect on flux of blocking the PPP at the transaldolase step. As expected, in the absence of labeled $^{13}C_1$-glucose, the observed $^{13}CO_2/^{12}CO_2$ ratio in both strains was the same (approximately -11.2 per mil VPDB). However, when 2% of the total glucose was labeled with $^{13}C_1$-glucose, the $^{13}CO_2/^{12}CO_2$ ratio was found to be higher for the Gad+ strain, by 0.56 per mil VPDB, than for the control strain (**Table 2**). Although small, the

difference was greater than the detection limit of the IRMS (±0.05 per ml VPDB) and was statistically highly significant (p = 9.77x10^{-6}, Student's 2-sided T-test) (**Table 3**). This difference of 0.56 per mil VPDB corresponds to an increase of 2.5% in glucose flux through the PPP for the gadusol-producing yeast relative to the control.

Table 2. Mean $^{13}CO_2/^{12}CO_2$ ratios obtained for the control and Gad+ yeast strains.

Percentage of labeled $^{13}C_1$-glucose	$^{13}CO_2/^{12}CO_2$ per mil* Gad+	$^{13}CO_2/^{12}CO_2$ per mil* Control	Difference in per mil* Gad/Control
0.00	-11.25 ± 0.029	-11.23 ± 0.033	0.02
2.00	-5.08 ± 0.018	-5.64 ± 0.025	0.56

*Isotope measurement in units of per mil VPDB

Table 3. $^{13}CO_2/^{12}CO_2$ ratios observed in each replicate for which the means are provided in Table 2.

Vial	$^{13}CO_2/^{12}CO_2$ per mil* Gad+	$^{13}CO_2/^{12}CO_2$ per mil* Control
1a	-5.169	-5.652
1b	N/A	-5.694
2a	-4.951	-5.698
2b	-4.969	-5.737
3a	-5.077	-5.623
3b	-5.105	-5.591

*Isotope measurement in units of per mil VPDB

Why wasn't a greater change observed in $^{13}CO_2/^{12}CO_2$ ratio between the Gad+ and the control strain? One explanation is that gadusol formation by the same Gad+ strain during log phase is much lower than during stationary phase (Figure 9; Osborn *et al*., 2015). The measurements in the present experiments were also taken during log phase. According to **Figure 9**, less than 10 µM gadusol was produced by the Gad+ strain during log phase. In contrast, the gadusol concentration increased to 100 µM during stationary phase. Therefore, it is possible that little difference in

glucose flux occurred between the control and Gad+ strains when the headspace gas samples were taken. It is likely that both the control and Gad+ strains were metabolizing maximal amounts of glucose through the PPP during log phase in order to satisfy growth needs. That is, the generation of the PPP intermediate ribose 5-phosphate needed for the synthesis of purines for RNA and DNA biosynthesis and amino acids for protein synthesis was occurring at about the same rate for both strains. Had samples been taken during stationary phase, they would have at least corresponded to the time when gadusol formation was previously observed to be significant (Osborn *et al*., 2015). An alternative explanation is that both the control and Gad+ strains contained a second but poorly characterized transaldolase gene called *NQM1* that was still active, meaning that the PPP was not completely blocked in the two strains. It is likely therefore, that residual transaldolase activity due to the *NQM1* gene reduced flux of sedoheptulose 7-phosphate through the Gad+ shunt pathway. On-going work in the Bakalinsky laboratory to knock out function of *NQM1* in both strains will allow direct determination of this possibility.

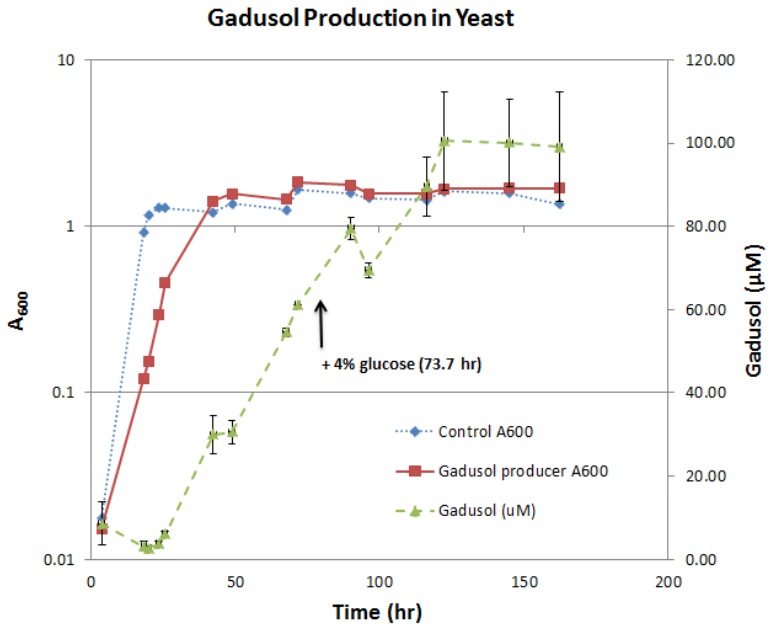

Figure 9. Gadusol production in yeast (Osborn *et al*., 2015). Gadusol concentration increased from about 30 μM when cells stopped growing, to about 110 μM at 120 hours.

Supplementary Chapter:
FDA versus the European Commission: A Comparison of Sunscreen Regulations

1. Sunscreen products are regulated in the U.S. by the FDA

1.1. Sunscreen products are regulated as over-the-counter drugs

The U.S. Food and Drug Administration (FDA) considers all sunscreen products over-the-counter (OTC) or nonprescription drugs. According to the Federal Food, Drug, and Cosmetic Act, drugs are defined as any "articles intended for use in the diagnosis, cure, mitigation, treatment, or prevention of disease" and "articles (other than food) intended to affect the structure or any functions of the body of man or other animals" (FD&C Act, sec. 201). Any product containing an ingredient with a known therapeutic use, such as fluoride in toothpaste, makes the product a drug. Any product with a claim that states its intended use is to treat or prevent disease, or otherwise affect the structure or functions of the human body, will also be considered a drug even if the product is marketed under a different category. For example, if a fragrance, normally labeled as a cosmetic, is marketed with "aromatherapy" claims, the fragrance then meets the definition of a drug because of its intended use. Thus, a sunscreen product with multiple therapeutic ingredients and claims stating an intended use for protection against ultraviolet radiation will be considered a drug.

Because all sunscreen products are OTC drugs, any new sunscreen ingredient under review must either conform to existing OTC drug monographs, which are developed and published in the *Federal Register* by the FDA, or follow a New Drug Application process. An OTC drug monograph is a "recipe book" for established FDA regulations covering acceptable ingredients, doses, formulations, and labeling information. These monographs, specific to each drug class, define the safety, effectiveness, and labeling of all marketed active ingredients in OTC drugs. New sunscreen products that do not conform to the OTC drug monographs are required to follow a New Drug Application process. This process requires products to have FDA pre-market approval, and to

follow mandated FDA review timelines. In contrast to new products using FDA-approved sunscreen ingredients, new (or existing) products using new sunscreen ingredients will be reviewed as a new drug. Products subjected to clinical studies by the FDA must include studies on consumer label comprehension and correct usage of the new products as directed by instruction labels.

1.2. Why the FDA is unlikely to approve new sunscreen ingredients

The FDA subjects a New Drug Application to a lengthy review process. With eight new and advanced European sunscreen ingredients waiting to be reviewed by the FDA, dermatologists and advocates for patients with melanoma – a form of skin cancer – formed a coalition called Public Access to Sunscreens (PASS) to lobby Congress to pass the Sunscreen Innovation Act. The act, signed into law in 2014, established an expedited process for the review and approval of OTC sunscreens. As a result, the FDA was forced to respond to the pending applications of the eight European sunscreen ingredients: amiloxate, bemotrizinol, bisoctrizole, drometrizole trisiloxane, ecamsule, enzacamene, iscotrizinol, and octyl triazone, some of which have been awaiting an FDA response since 2002 (Reisch *et al*., 2015). The law did not require the FDA to approve of the eight sunscreen ingredients, only to review and respond to their respective applications. Upon review, the FDA rejected all eight sunscreen ingredients due to a lack of additional data to rule out risks from chronic exposure in pregnant women and children.

According to the director of FDA's Division of Nonprescription Drug Products, the FDA "needs more data to decide if these ingredients are, in fact, generally recognized as safe and effective for use in OTC sunscreen products" (Reisch *et al*., 2015). Although these sunscreen ingredients have been commercially available to European consumers for the past five years, the FDA still lacks scientific data on their long-term effects and on the amount of ingredient absorption that occurs during use. Following rejection of all eight sunscreen ingredients, the PASS coalition

stated that the FDA "demonstrated clear disregard for the increased rates of melanoma and the public's demand for the latest sunscreen technology" (Sharfstein *et al*., 2015). However, given the lack of scientific evidence, it appears that the FDA was forced to act cautiously, in part, because sunscreen products are regulated as OTC drugs, and in part, due to the risk of liability in the event of an adverse reaction involve use of these sunscreen ingredients. In order for the FDA to approve use of the ingredients, current law regarding review of new OTC drug products would have to be changed.

2. Sunscreen products are regulated in the EU by the European Commission

2.1. Sunscreen products are regulated as cosmetics

In Europe, the European Commission (EC) regulates all sunscreen products as cosmetics. The EC defines a cosmetic as "any substance or preparation intended to be placed in contact with the various external parts of the human body or with the teeth and the mucous membranes of the oral cavity with a view exclusively or mainly to cleansing them, perfuming them, changing their appearance and/or correcting body odors and/or protecting them or keeping them in a good condition" (Official Journal of European Union, 2006). Thus, products like toothpaste are considered cosmetics in Europe, as opposed to OTC drugs. Although sunscreen products are designed to protect against dangerous UV radiation, sunscreen products in Europe cannot make the following claims due to the regulations that apply to cosmetics: "100% protection from UV radiation," such as "sunblock" or "total protection," or "no need to re-apply the product under any circumstances," such as "all day prevention" (Official Journal of the European Union, 2006). In addition, sunscreen products must include warnings stating that they do not provide 100% sunscreen protection.

According to current cosmetic regulations, the EC requires new cosmetic products in the EU to be registered in the Cosmetic Products Notification Portal before marketed, and makes EU countries responsible for market surveillance at the national level. As in the U.S., the manufacturer is responsible for the safety of the products, meaning that the manufacturer must perform all necessary scientific safety assessments before products are marketed. However, the EC does not specify any testing requirements for cosmetic products or ingredients. Instead of OTC monographs, the EC has a special database, called CosIng, which specifies the legal requirements and restrictions on cosmetic substances and ingredients.

According to the EC sunscreen regulations, new sunscreen products must contain protection against both UVB (290-320 nm) and UVA (320-400nm) radiation. The minimum degree of protection required by the EC against UVB and UVA is defined in terms of a sunscreen protection factor (SPF). SPF is the "ratio of minimum erythemal dose (minimal radiation dose that may produce sunburn) on skin protected by a sunscreen product to the minimum erythemal dose on the same unprotected skin" (Official Journal of the European Union, 2006). Sunscreen products must contain a minimum protection against UVB of SPF 6 and minimum protection against UVA equal to 1/3 of the UVB SPF (Official Journal of the European Union, 2006). Because sunscreen products are regulated as cosmetics, the approval process for new sunscreen products is faster and less strict than in the U.S. where sunscreen products are regulated as OTC drugs.

3. Differences between cosmetic and OTC drug regulations in the U.S. and Europe

The FDA defines cosmetics as "articles intended to be rubbed, poured, sprinkled, or sprayed on, introduced into, or otherwise applied to the human body for cleansing, beautifying, promoting attractiveness, or altering the appearance." Based on this definition, some products can be considered both cosmetics and drugs. For example, an anti-dandruff shampoo is both a cosmetic

and drug because the intended use is to cleanse and treat dandruff. However, unlike pharmaceutical drugs, the FDA does not pre-approve cosmetic products or ingredients, with the exception of color additives. As in Europe, U.S. regulations do not specify any particular testing regimens for cosmetic products or ingredients. Rather, it is the manufacturers' responsibility to substantiate product and ingredient safety prior to marketing.

In Europe, OTC pharmaceutical classifications differ for each country, and therefore OTC drug regulations vary across the continent. However, procedures exist that allow for mutual recognition of OTC products. This enables manufacturers to seek simultaneous marketing authorization in two or more European countries, provided that the drug is authorized in at least one (Bond *et al*., 2004). In general, OTC drug regulations in Europe are stricter than cosmetic regulations.

4. Gadusol as a new sunscreen ingredient in skincare products

I speculate that the sunscreen compound, gadusol, would be more likely to be approved by the EC than by the FDA because of the cosmetic classification of sunscreen products in Europe. Cosmetics, both in Europe and the U.S., are subject to less strict regulation than drugs. Because sunscreen products are considered OTC drugs in the U.S., new sunscreen ingredients face greater difficulties in entering the U.S. market due to stricter regulation by the FDA.

Appendix A – Expected CO_2 production by yeast

As described in the Preliminary Experiments section in the Results and Discussion on p. 12-14, yeast growth rate was estimated over an approximate 100-hour time course by measuring weight loss of a vented fermentation vessel containing 19 ml of a yeast medium inoculated with either the control strain or the Gad+ strain and incubated statically at 30°C. The following calculation shows the amount of CO_2 that would be produced assuming that all the sugar in the medium was fermented by the yeast to CO_2 and ethanol. Because the CO_2 was vented to the atmosphere, the measured loss in weight of the vessel was expected to correspond to the amount of CO_2 lost. The cultures contained 19 ml of medium which consisted of YNB + 2% glucose. For every mole of glucose consumed by yeast during glycolysis (fermentation), 2 moles of ethanol and 2 moles of CO_2 are produced.

Glycolysis:

$C_6H_{12}O_6$ (glucose) → 2 C_2H_6O (ethanol) + 2 CO_2

1. Expected mass of CO_2 that would be produced from a **19 mL culture**:

$$0.38 \text{ g glucose} \times \frac{\text{mol glucose}}{180.2 \text{ g glucose}} \times \frac{2 \text{ mol } CO_2}{\text{mol glucose}} \times \frac{44 \text{ g}}{\text{mol } CO_2} = \mathbf{0.185 \text{ g } CO_2}$$

2. Expected volume of CO_2 that would be produced from a **19 mL culture**:

$$\mathbf{Volume\ of\ CO_2} = \mathbf{0.185 \text{ g } CO_2} \times \frac{\text{mol } CO_2}{44 \text{ g}} \times \frac{22.4 \text{ L}}{\text{mol } CO_2} = \mathbf{95 \text{ mL } CO_2}$$

Observations

The measured weight loss after about 100 hours for the control fermentation was 0.191 g, which corresponds well to the expected 0.185 g. The measured weight loss for the Gad+ strain was 0.246 g or about 30% higher than for the control strain. (The experiment was performed in duplicates. The values for the control were 0.194 and 0.189 g and 0.246 and 0.246 g for the Gad+ strain.) Even more important than determining the final weight loss, a sufficient amount of CO_2 was produced at the start (~20 hours post-inoculation) and during exponential phase of growth for this period to be monitored accurately. This was important because CO_2 had to be collected during the exponential phase of growth in the experimental cultures.

Appendix B – Theoretical $^{13}CO_2/^{12}CO_2$ levels in the control and Gad+ strains fed $^{13}C_1$-glucose

Previous work has estimated glucose flux through the pentose phosphate pathway (PPP) in glucose-limited chemostat cultures of *S. cerevisiae* based on metabolic flux analysis. Under anaerobic conditions, Nissen *et al*., 1997, found that 10% of the glucose was catabolized in a prototrophic haploid strain via the PPP and 90% via glycolysis based on measured enzyme activities, independent of dilution rate. The calculated split was found to be 6.3% via the PPP and 93.7% via glycolysis at a low dilution rate, and 7.7% via the PPP and 92.3% via glycolysis at a high dilution rate. Using a prototrophic diploid strain under aerobic conditions, van Winden *et al*., 2005 found that 24% of the glucose was catabolized via the PPP and 76% via glycolysis.

The following calculations predict $^{13}CO_2/^{12}CO_2$ ratios produced by the control and Gad+ strains grown on $^{13}C_1$-glucose, based on 6.3% or 24% of the glucose being metabolized via the pentose phosphate pathway, as calculated by Nissen *et al.* (1997) or measured by van Winden *et al.* (2005), respectively.

It is important to note that while these calculations determine actual $^{13}CO_2/^{12}CO_2$ ratios, the IRMS instrument determined "VPDB $^{13}CO_2/^{12}CO_2$ ratios." The two values are not directly comparable. However, in theory, it is possible to convert the latter values to actual values if the absolute $^{13}CO_2$ composition of the reference CO_2 gas (acidified NBS19 calcium carbonate powder) is known.

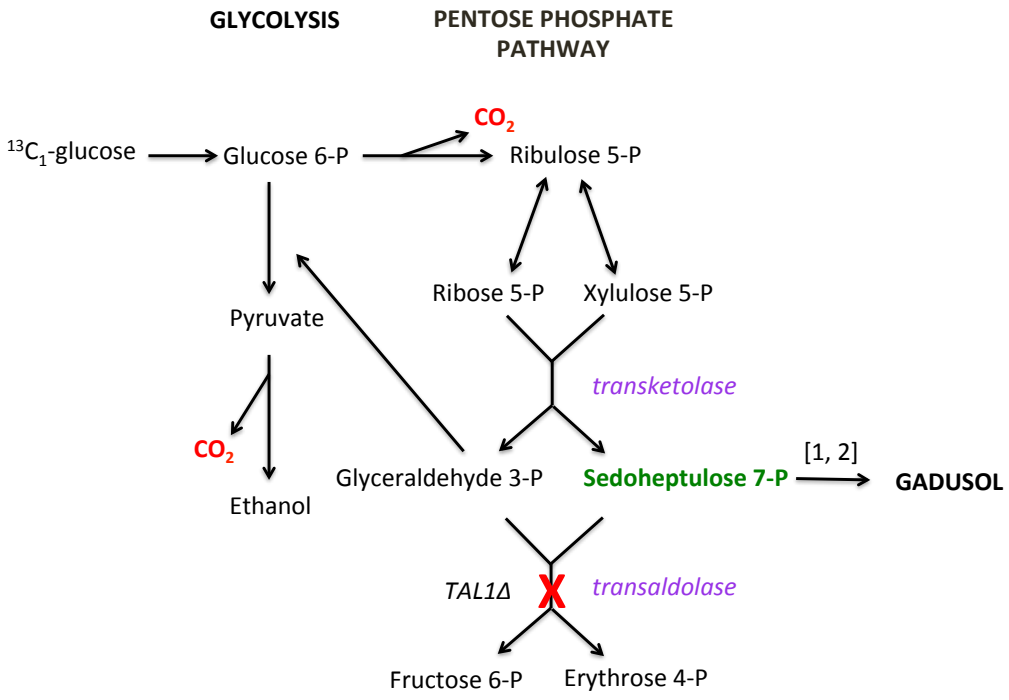

Figure 10. Abbreviated glycolytic and the pentose phosphate pathways (PPP) in the *tal1*Δ mutant of *S. cerevisiae*. Glyceraldehyde 3-phosphate generated at the transketolase step in the PPP can re-enter glycolysis. The Gad+ strain has the gadusol biosynthetic genes [1, 2] while the control strain does not.

As noted earlier, the CO_2 produced in the PPP is derived exclusively from the C_1 carbon of glucose, whereas the CO_2 produced in glycolysis is derived from the C_3 and C_4 carbons. **Figure 10** shows production of CO_2 in the control and Gad+ strains (both *tal1*Δ mutants) grown on $^{13}C_1$-glucose. No $^{13}CO_2$ is produced via glycolysis, whereas for every glucose catabolized via the PPP, one $^{13}CO_2$ is produced. Because the glyceraldehyde 3-phosphate generated in the transketolase step in the PPP can re-enter glycolysis, it generates an additional $^{12}CO_2$.

Thus, for every $^{13}C_1$-glucose molecule catabolized via glycolysis, two $^{12}CO_2$ molecules are produced. To follow carbon flow through the PPP, **Figure 10** shows two $^{13}C_1$-glucose molecules entering the pathway but indicates net CO_2 production per $^{13}C_1$-glucose molecule in the final equation. For every $^{13}C_1$-glucose catabolized via the PPP, one $^{13}CO_2$ and ½ $^{12}CO_2$ are generated. The $^{13}CO_2$ is generated from the decarboxylation of gluconate 6-P and the $^{12}CO_2$ is generated from the glyceraldehyde 3-phosphate that re-enters glycolysis.

Although the calculated stoichiometry is the same for both the control and Gad+ strains, we speculate that in the control strain lacking the Gad+ shunt, glucose flux through the PPP will be slowed.

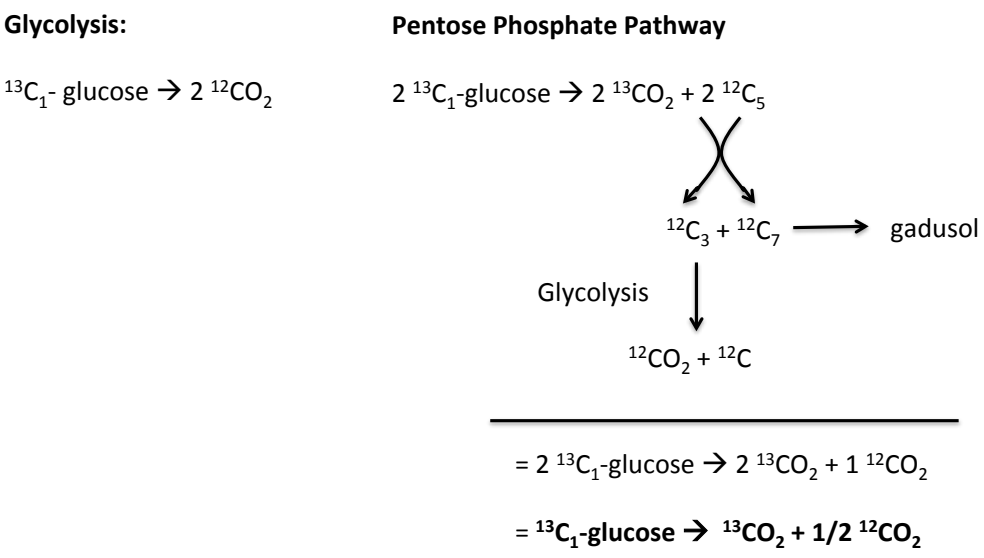

Figure 11. CO_2 produced via catabolism of $^{13}C_1$-glucose in glycolysis and in the PPP.

$^{13}C_1$-glucose catabolism to CO_2 in the control and Gad+ strains

1. Calculation based on van Winden *et al.,* 2005

Assumptions
A. 24% of the glucose is catabolized via the PPP and 76% is catabolized via glycolysis.
B. All the glucose fed to the yeast is $^{13}C_1$-glucose.
C. 10% of the glucose catabolized via glycolysis is assimilated into new cell mass and therefore does not produce CO_2.

The amount of $^{13}CO_2$ produced per molecule of glucose:
$^{13}CO_2 = 0.24$

The amount of $^{12}CO_2$ produced per molecule of glucose:
From the PPP: $^{12}CO_2 = (0.24)(1/2) = 0.12$
From glycolysis: $^{12}CO_2 = (0.76)(0.90)(2) = 1.368$
Total $^{12}CO_2 = 1.49$

The $^{13}CO_2/^{12}CO_2$ ratio = 0.24/1.64 = **0.161**

Taking into consideration that only 2% of the total glucose was labeled with $^{13}C_1$-glucose, the ratio becomes:
$^{13}CO_2/^{12}CO_2 = (0.02)(0.161) = 3.22x10^{-3}$

2. Calculation based on Nissen *et al.,* 1997

Assumptions
A. 6.3% of the glucose is catabolized via the PPP and 93.7% is catabolized via glycolysis.
B. All the glucose fed to the yeast is $^{13}C_1$-glucose.
C. 10% of the glucose catabolized via glycolysis is assimilated into new cell mass and therefore does not produce CO_2.

The amount of $^{13}CO_2$ produced per molecule of glucose:
$^{13}CO_2 = 0.063$

The amount of $^{12}CO_2$ produced per molecule of glucose:
From the PPP: $^{12}CO_2 = (0.063)(1/2) = 0.032$
From glycolysis: $^{12}CO_2 = (0.937)(0.90)(2) = 1.687$
Total $^{12}CO_2 = 1.70$

The $^{13}CO_2/^{12}CO_2$ ratio = 0.063/1.70 = **0.037**

Taking into consideration that only 2% of the total glucose was labeled with $^{13}C_1$-glucose, the ratio becomes:
$^{13}CO_2/^{12}CO_2 = (0.02)(0.037) = 7.39x10^{-4}$

References:

Berg, J. M., Tymoczko J.L., Stryer, H. (2012). *Biochemistry*. 7th.

Bond, C.M., Orru, M.P., Leder, J.M., Bouvy, M. (2004). *Regulating pharmaceuticals in Europe: striving for efficiency, equity, and quality*, E. Mossialos, M. Mrazek, T. Walley, eds., Open University Press, England.

European Commission. (2006). Commission Recommendation. *Official Journal of the European Union 265*, 39-43.

FDA. (2014). Cosmetics & U.S. Law. *U.S. Food and Drug Administration*.

FDA. (2014). Drug Applications for Over-the-Counter (OTC) Drugs. *U.S. Food and Drug Administration*.

Fraenkel, D. G. (1982). Carbohydrate metabolism, p. 1-37, In: *The Molecular Biology of the Yeast Saccharomyces, Metabolism and Gene Expression*, J.N. Strathern, E.W. Jones, J.R. Broach, eds., Cold Spring Harbor Press, NY.

Jordaan, M., Laurens, J.B. (2008). Diagnosis of *Helicobacter pylori* infection with the ^{13}C-urea breath test by means of GC-MS analysis. *J. Sep. Science 31*, 329-335.

Katz, J., Abraham, R.H., Chaikoff, I.L. (1955). The occurrence and mechanism of the hexose monophosphate shunt in rat liver slices. *J. Biol. Chem. 214,* 853-868.

Muccio, Z., and Jackson, P. G. (2009). Isotope ratio mass spectrometry. *Analyst 134*, 213-222.

Nissen, T. L., Schulze, U., Nielsen, J., Villadsen, J. (1997). Flux distributions in anaerobic, glucose-limited continuous cultures of *Saccharomyces cerevisiae*. *Microbiol. 143*, 203-218.

Osborn, A., Almabruk, K., Holzwarth, G., Asamizu, S., Ladu, J., Kean, K. M., Karplus, A., Tanguay, R.L., Bakalinsky, A. T., Mahmud, T. (2015). De novo synthesis of a sunscreen compound in vertebrates. *eLife 4,* 1-15

Reisch, M. S. (2015) After More Than A Decade, FDA Still Won't Allow New Sunscreens. *Amer. Chem. Soc. 93*, 10-15.

Sharfstein, J. M. (2015). A Spotlight on Sunscreen Regulation. *New England J. Med. 373*, 101-103.

Toya, Y., Kono N., Arakawa, K., Tomita, M. (2011). Metabolic Flux Analysis and Visualization. *J. Proteome R. 10*, 3313-3323.

van Winden, W.A., van Dam, J.C., Ras, C., Kleijn, R.J., Vinke, J.L., Gulik W.M., Heijnen, J.J.(2005). Metabolic-flux analysis of *Saccharomyces cerevisiae* based on mass isotopomer measurements of ^{13}C-labeled primary metabolites. *FEMS Yeast Research 5*, 559-568.

Zabielski, P., Ford G.C., Persson, X.M., Jaleel, A., Dewey, J.D., Nair K. S. (2013). Comparison of different mass spectrometry techniques in the measurement of L-[ring-$^{13}C_6$]phenylalanine incorporation into mixed muscle proteins. *J. Mass Spectrom 48*, 269-275.